

**SOLUBILITY OF CARBON DIOXIDE
IN FIVE PROMISING IONIC LIQUIDS**

Thanawat Nonthanasin


A Thesis Submitted in Partial Fulfilment of the Requirements
for the Degree of Master of Science
The Petroleum and Petrochemical College, Chulalongkorn University
in Academic Partnership with
The University of Michigan, The University of Oklahoma,
Case Western Reserve University, and Institut Français du Pétrole
2013

I28372232

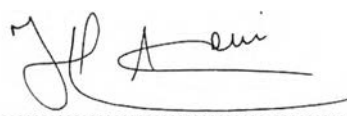
561600


Thesis Title: Solubility of Carbon Dioxide in Five Promising Ionic Liquids
By: Thanawat Nonthanasin
Program: Petrochemical Technology
Thesis Advisors: Prof. Amr Henni
Assoc. Prof. Chintana Saiwan

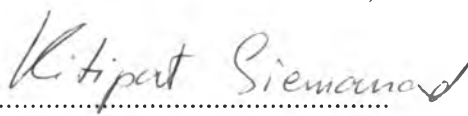
Accepted by The Petroleum and Petrochemical College, Chulalongkorn University, in partial fulfilment of the requirements for the Degree of Master of Science.

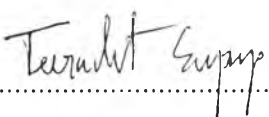

..... College Dean
(Asst. Prof. Pomthong Malakul)

Thesis Committee:


.....
(Prof. Amr Henni)


.....
(Assoc. Prof. Chintana Saiwan)


.....
(Asst. Prof. Kitipat Siemanond)


.....
(Dr. Teeradet Supap)

บทคัดย่อ

ธนวัฒน์ นนทธรสิน: ความสามารถในการละลายของคาร์บอนไดออกไซด์ในไอออนิกลิควิด 5 ชนิด (Solubility of Carbon Dioxide in Five Promising Ionic Liquids) อ. ที่ปรึกษา: ศ. ดร. อามาร์ เชนี และ รศ. ดร. จินตนา สายวรรณ 204 หน้า

ในปัจจุบัน ไอออนิกลิควิดเป็นตัวทำละลายสำหรับกระบวนการจับคาร์บอนไดออกไซด์ที่ประหยัดพลังงานและเป็นมิตรต่อสิ่งแวดล้อมมากที่สุด งานวิจัยนี้มุ่งเน้นที่การวัดความสามารถในการละลายของคาร์บอนไดออกไซด์ในไอออนิกลิควิดที่อุณหภูมิห้องทั้ง 5 ชนิด ได้แก่ ไตรเอทิลซัลโฟนิล บิส(ไตรฟลูออโรเมทิลซัลโฟนิล)อีไมด์ ($[S_{222}][Tf_2N]$), ไดเอทิลเมทิล(ทู-เมทอกซีเอทิล)แอมโมเนียม บิส(ไตรฟลูออโรเมทิลซัลโฟนิล)อีไมด์ ($[deme][Tf_2N]$), วัน-โพรพิล-ทรี-เมทิลอิมิดาโซเลียม บิส(ไตรฟลูออโรเมทิลซัลโฟนิล)อีไมด์ ($[pmim][Tf_2N]$), วัน-แอลลีล-ทรี-เมทิลอิมิดาโซเลียม บิส(ไตรฟลูออโรเมทิลซัลโฟนิล)อีไมด์ ($[amim][Tf_2N]$) และ วัน-บิลทิล-โพร-เมทิลไพริดีเนียม เตตระฟลูออโรโบเรต ($[4mbp][BF_4]$) ที่อุณหภูมิ 313.15, 323.15 และ 333.15 K ภายใต้ความดัน 20 บาร์ โดยใช้เครื่องไมโครบาลานซ์ ชนิดกราวเมตริก ค่าความสามารถในการละลายของคาร์บอนไดออกไซด์ในตัวทำละลายเหล่านี้ที่ได้จากการทดลองสัมพันธ์กับสมการสถานะเพง-โรบินสันมาตรฐาน, สมการสถานะซอว์-เรดลิก-ควงมาตรฐาน, สมการสถานะซอว์-เรดลิก-ควงที่ใช้กฎการผสมแบบควอดราติก, และแบบจำลองสัมประสิทธิ์เอกทิวิตีของ NRTL ด้วยค่าความคลาดเคลื่อนสัมบูรณ์เฉลี่ย (AADs) ที่น่าพึงพอใจ งานวิจัยนี้ได้หาค่าพารามิเตอร์อันตรกิริยาสำหรับสมการสถานะและแบบจำลองสัมประสิทธิ์เอกทิวิตีอีกด้วย จากการทดลองพบว่าการดูดซึมของคาร์บอนไดออกไซด์มีแนวโน้มลดลงตามลำดับดังนี้ $[deme][Tf_2N] > [pmim][Tf_2N] > [amim][Tf_2N] > [S_{222}][Tf_2N] > [4mbp][BF_4]$ ไอออนิกลิควิด 4 ชนิด $[deme][Tf_2N]$, $[pmim][Tf_2N]$, $[amim][Tf_2N]$, and $[S_{222}][Tf_2N]$ ถือว่าเป็นตัวทำละลายที่เป็นทางเลือกสำหรับกระบวนการจับคาร์บอนไดออกไซด์เนื่องจากการดูดซึมคาร์บอนไดออกไซด์ที่สูง ซึ่งสามารถเปรียบเทียบได้กับไอออนิกลิควิดอื่นๆ ที่แสดงการดูดซึมทางกายภาพในลักษณะเดียวกันที่น่าสนใจกว่านั้นคือ $[deme][Tf_2N]$ แสดงความสามารถในการละลายของคาร์บอนไดออกไซด์ที่สูงที่สุดอย่างเห็นได้ชัดในกลุ่มไอออนิกลิควิดชนิดแอมโมเนียม นอกจากนี้ วิทยานิพนธ์ฉบับนี้ยังได้นำเสนอค่าคงที่ของเฮนรี เอนทาลปีและเอนโทรปีของการดูดซึมคาร์บอนไดออกไซด์ในไอออนิกลิควิดที่ศึกษาอีกด้วย

ABSTRACT

5471025063: Petrochemical Technology Program
 Thanawat Nonthanasin: Solubility of Carbon Dioxide in Five
 Promising Ionic Liquids
 Thesis Advisor: Prof. Amr Henni and Assoc. Prof. Chintana Saiwan
 204 pp.

Keywords: Ionic liquids/ CO₂ capture/ CO₂ solubility/ PR/ SRK/ NRTL/
 Henry's law constant/ Enthalpy and entropy of absorption

Ionic liquids are presently considered the most energy-efficient and environmentally benign solvents for CO₂ capture. This research aimed at measuring the solubility of CO₂ in five room temperature ionic liquids, triethylsulfonium bis(trifluoromethylsulfonyl)imide ([S₂₂₂][Tf₂N]), diethylmethyl(2-methoxyethyl)-ammonium bis(trifluoromethylsulfonyl)imide ([deme][Tf₂N]), 1-propyl-3-methylimidazolium bis(trifluoromethylsulfonyl)imide ([pmim][Tf₂N]), 1-allyl-3-methylimidazolium bis(trifluoromethylsulfonyl)imide ([amim][Tf₂N]), and 1-butyl-4-methylpyridinium tetrafluoroborate ([4mbp][BF₄]) at (313.15, 323.15 and 333.15 K) and at pressure up to 20 bar using a gravimetric microbalance. The experimental solubility data of CO₂ in these solvents were well correlated using the standard Peng-Robinson (PR-EoS), the standard Redlich-Kwong-Soave (SRK-EoS), the SRK-EoS with quadratic mixing rules, and the Non-Random Two-Liquid (NRTL) with satisfactory average absolute deviations (AADs). Binary interaction parameters for these correlations were obtained. The absorption of CO₂ was prone to diminish in this sequence: [deme][Tf₂N] > [pmim][Tf₂N] > [amim][Tf₂N] > [S₂₂₂][Tf₂N] > [4mbp][BF₄]. Four ionic liquids, [deme][Tf₂N], [pmim][Tf₂N], [amim][Tf₂N], and [S₂₂₂][Tf₂N], are deemed promising due to comparably high CO₂ absorption with physical absorption to other prevalent CO₂-absorbing ionic liquids. More interestingly, [deme][Tf₂N] evidently had the highest CO₂ solubility among all ammonium-based ionic liquids reported in the literature. In addition, Henry's law constants and enthalpies and entropies of absorption for CO₂ in the investigated ionic liquid are also reported.

ACKNOWLEDGEMENTS

I would like to express my wholehearted gratitude to Prof. Amr Henni, my advisor, for giving me an unforgettable opportunity to conduct this research and providing financial supports to me during my stay at the University of Regina. His willingness to devote his time so generously to give me his valuable suggestions and to correct my works has been very much appreciated. Special thanks are also given to Assoc. Prof. Chintana Saiwan, my co-advisor, for her professional guidance, and enthusiastic encouragement. My grateful thanks are extended to Asst. Prof. Kitipat Siemanond and Dr. Teeradet Supap as my thesis committees.

For my research group members, I would really like to extend my appreciation to Kazi Zamshad Sumon and Tursun John Uygur as my trainers for the experimental set-up and procedures. Also, I wish to thank Mohamed Zoubeik and Vasantha Raja Ramamoorthy as my sincere friends as well as their useful advices and discussion. I would also like to acknowledge and thank the University of Regina staffs who buttressed me from beginning through completion: Christine Barlow, Jill Docking, Robyn Fahlman and Melissa Dyck.

I wish to express my acknowledgement to International Test Centre for CO₂ Capture, Petroleum Technology Research Centre, University of Regina, also The Petroleum and Petrochemical College, and the National Center of Excellence for Petroleum, Petrochemicals, and Advanced Materials, Thailand for the grant and funding support.

For a good life of living in Canada, I would like to give my thanks to my nice friends coming together with me, Wirit Cuptasanti and Wantanee Teerasukakul, for their helps in many things. Moreover, I am indeed thankful to the members of Student Association of Thais at the University of Regina (SATUR), namely, Chitsutha Soomlek, Yanee Lertnimoolchai, Wayuta Srisang, Jarotwan Koiwanit, Suriya Jirasatitsin, Kriengkamol Setameteekul, Wisan Sila, Wasin Sananphanichkul, Wichitpan Rongwong, and all of my friends in Regina who gave me assistance and unforgettably memorable experiences.

Finally, I feel overwhelmingly grateful to my parents for their support and encouragement throughout my study. Thank you very much.

TABLE OF CONTENTS

	PAGE
Title Page	i
Abstract (in English)	iii
Abstract (in Thai)	iv
Acknowledgements	v
Table of Contents	vi
List of Tables	x
List of Figures	xv
 CHAPTER	
I INTRODUCTION	1
 II LITERATURE REVIEW	
2.1 Ionic Liquids	4
2.2 Physical Properties	7
2.2.1 Melting Point	8
2.2.2 Density	10
2.2.3 Viscosity	12
2.2.4 Vapor Pressure	16
2.2.5 Thermal Stability	18
2.2.6 Surface Tension	20
2.2.7 Miscibility with Water	23
2.3 Uses and Applications	24
2.4 Methods for Measuring Gas Solubilities	25
2.4.1 Stoichiometric Technique	26
2.4.2 Pressure Drop Technique	27
2.4.3 Gravimetric Methods	28
2.5 Classification of Ionic Liquids for CO ₂ Capture	31
2.6 CO ₂ Solubility in Conventional Ionic Liquids	32
2.6.1 Effect of Pressure and Temperature on CO ₂ Solubility	48

CHAPTER	PAGE
2.6.2 Effect of Structural Variation on CO ₂ Solubility	51
2.6.2.1 Anion Effect	51
2.6.2.2 Cation Effect	53
2.7 Thermodynamic Modeling	54
2.7.1 Group Contribution Methods for Critical Properties	54
2.7.2 Equations of State (EoS)	57
2.7.2.1 The Standard Redlich-Kwong-Soave (SRK-EoS)	59
2.7.2.2 The Standard Peng-Robinson (PR-EoS)	60
2.7.2.3 The Redlich-Kwong-Aspen (The SRK with Quadratic Mixing Rules)	62
2.7.3 Activity Coefficient Model	63
2.7.3.1 The Non-Random Two-Liquid (NRTL)	63
2.8 Derivation of Henry's law constant	65
2.9 Derivation of Enthalpies and Entropies of Absorption	67
 III EXPERIMENTAL	 69
3.1 Materials	69
3.1.1 Ionic Liquids	69
3.1.2 Gases	72
3.2 Experimental Procedures	72
3.2.1 Density Measurement	72
3.2.2 Gas Solubility Measurement	73
3.2.2.1 Preparation of Sample, Accessories and Program	76
3.2.2.2 Sample Loading	77
3.2.2.3 New Application Set-up	78
3.2.2.4 Drying and degassing	78
3.2.2.5 Isotherm	79
3.2.2.6 Sample Removal	79

CHAPTER	PAGE
3.2.3 Buoyancy Correction and Data Treatment	80
IV RESULTS AND DISCUSSION	84
4.1 Density of Pure Ionic Liquids	84
4.2 Solubility of Carbon Dioxide	87
4.2.1 Experimental Solubility Isotherms	87
4.2.2 Effects of Temperature and Pressure	90
4.2.3 Effects of Cations and Anions	91
4.2.4 Comparison with Ionic Liquids in Our Group	102
4.3 Thermodynamic Modeling	103
4.3.1 Critical Property Estimation	103
4.3.2 Equations of State	104
4.3.2.1 The Standard Peng-Robinson (PR-EoS)	105
4.3.2.2 The Standard Redlich-Kwong-Soave (SRK-EoS)	110
4.3.2.3 The Redlich-Kwong-Soave (SRK) with Quadratic Mixing Rules	114
4.3.3 Activity Coefficient Model	119
4.3.3.1 The Non-Random Two-Liquid (NRTL)	119
4.4 Henry's Law Constants and Enthalpies and Entropies of Absorption	124
4.4.1 Henry's Law Constants	124
4.4.2 Enthalpies and Entropies of Absorption	126
V CONCLUSIONS AND RECOMMENDATIONS	128
REFERENCES	130

CHAPTER	PAGE
APPENDICES	143
Appendix A Raw Data for Gas Solubility Measurements Using The Gravimetric Microbalance	143
Appendix B Critical Property Estimation	159
Appendix C Consistency Test of Densities	164
Appendix D Modeling Results with The AADs	169
Appendix E Henry's Law Constants and Enthalpies and Entropies of Absorption	184
CURRICULUM VITAE	204

LIST OF TABLES

TABLE	PAGE	
2.1	Melting points data for several ionic liquids	9
2.2	Densities (25 °C) of several ionic liquids Chromatography	11
2.3	Viscosity data (25 °C) for various ionic liquids	16
2.4	Thermal decomposition temperatures of several ionic liquids	20
2.5	Surface tension data (25 °C) for several ionic liquids	21
2.6	Literature surveys for the solubility of CO ₂ in numerous ionic liquids	35
2.7	Groups considered for the Modified Lydersen-Joback-Reid method and equations describing the model	56
3.1	Studied ionic liquids	71
3.2	Microbalance components for buoyancy correction	82
4.1	Experimental densities of the five ionic liquids measured at 1.01325 bar	86
4.2	Temperature-dependent density correlations for the studied ionic liquids	87
4.3	Experimental solubility (P, T, x) data for [S ₂₂₂][Tf ₂ N] (1) + CO ₂ (2), [deme][Tf ₂ N] (1) + CO ₂ (2), [pmim][Tf ₂ N] (1) + CO ₂ (2), [amim][Tf ₂ N] (1) + CO ₂ (2) and [4mbp][BF ₄] (1) + CO ₂ (2) systems at 313.15, 323.15 and 333.15 K	89
4.4	Molecular weights, normal boiling temperatures, critical properties, and acentric factors of ionic liquids	104
4.5	Binary interaction parameters of the standard PR-EoS for the ionic liquids (1) + CO ₂ (2) system	106
4.6	Average absolute deviation (AAD %) between experimental and estimated values of pressure by the standard PR-EoS for the ionic liquids + CO ₂ system	109

TABLE	PAGE
4.7 Binary interaction parameters of the standard SRK-EoS for the ionic liquids (1) + CO ₂ (2) system	110
4.8 Average absolute deviation (AAD %) between experimental and estimated values of pressure by the standard SRK-EoS for the ionic liquids + CO ₂ system	114
4.9 Binary interaction parameters of the SRK with quadratic mixing rules for the ionic liquids (1) + CO ₂ (2) system	115
4.10 Average absolute deviation (AAD %) between experimental and estimated values of pressure by the SRK with quadratic mixing rules for the ionic liquids + CO ₂ system	119
4.11 Binary interaction parameters of the NRTL for the ionic liquids (1) + CO ₂ (2) system ($\alpha = 0.3$)	120
4.12 Average absolute deviation (AAD %) between experimental and estimated values of pressure by the NRTL for the ionic liquids + CO ₂ system	124
4.13 Henry's law constants, enthalpies, and entropies of absorption for CO ₂ in the studied ionic liquids	125
A1 Carbon dioxide in [bmim][PF ₆] at 323.15 K	143
A2 Carbon dioxide in [S ₂₂₂][Tf ₂ N] at 313.15 K	144
A3 Carbon dioxide in [S ₂₂₂][Tf ₂ N] at 323.15 K	145
A4 Carbon dioxide in [S ₂₂₂][Tf ₂ N] at 333.15 K	146
A5 Carbon dioxide in [deme][Tf ₂ N] at 313.15 K	147
A6 Carbon dioxide in [deme][Tf ₂ N] at 323.15 K	148
A7 Carbon dioxide in [deme][Tf ₂ N] at 333.15 K	149
A8 Carbon dioxide in [pmim][Tf ₂ N] at 313.15 K	150
A9 Carbon dioxide in [pmim][Tf ₂ N] at 323.15 K	151
A10 Carbon dioxide in [pmim][Tf ₂ N] at 333.15 K	152
A11 Carbon dioxide in [amim][Tf ₂ N] at 313.15 K	153
A12 Carbon dioxide in [amim][Tf ₂ N] at 323.15 K	154

TABLE	PAGE
A13 Carbon dioxide in [amim][Tf ₂ N] at 333.15 K	155
A14 Carbon dioxide in [4mbp][BF ₄] at 313.15 K	156
A15 Carbon dioxide in [4mbp][BF ₄] at 323.15 K	157
A16 Carbon dioxide in [4mbp][BF ₄] at 333.15 K	158
B1 The normal boiling temperature, critical properties, and acentric factor of [S ₂₂₂][Tf ₂ N]	159
B2 The normal boiling temperature, critical properties, and acentric factor of [deme][Tf ₂ N]	160
B3 The normal boiling temperature, critical properties, and acentric factor of [pmim][Tf ₂ N]	161
B4 The normal boiling temperature, critical properties, and acentric factor of [amim][Tf ₂ N]	162
B5 The normal boiling temperature, critical properties, and acentric factor of [4mbp][BF ₄]	163
C1 The calculated density of [S ₂₂₂][Tf ₂ N] and comparison with the experimental values at a range of temperatures from 278.15 K to 353.15 K	164
C2 The calculated density of [deme][Tf ₂ N] and comparison with the experimental values at a range of temperatures from 278.15 K to 353.15 K	165
C3 The calculated density of [pmim][Tf ₂ N] and comparison with the experimental values at a range of temperatures from 278.15 K to 353.15 K	166
C4 The calculated density of [amim][Tf ₂ N] and comparison with the experimental values at a range of temperatures from 278.15 K to 353.15 K	167
C5 The calculated density of [4mbp][BF ₄] and comparison with the experimental values at a range of temperatures from 278.15 K to 353.15 K	168

TABLE	PAGE
D1 Modeling solubility (P, T, x) data for [S ₂₂₂][Tf ₂ N] (1) + CO ₂ (2) system at 313.15 K	169
D2 Modeling solubility (P, T, x) data for [S ₂₂₂][Tf ₂ N] (1) + CO ₂ (2) system at 323.15 K	170
D3 Modeling solubility (P, T, x) data for [S ₂₂₂][Tf ₂ N] (1) + CO ₂ (2) system at 333.15 K	171
D4 Modeling solubility (P, T, x) data for [deme][Tf ₂ N] (1) + CO ₂ (2) system at 313.15 K	172
D5 Modeling solubility (P, T, x) data for [deme][Tf ₂ N] (1) + CO ₂ (2) system at 323.15 K	173
D6 Modeling solubility (P, T, x) data for [deme][Tf ₂ N] (1) + CO ₂ (2) system at 333.15 K	174
D7 Modeling solubility (P, T, x) data for [pmim][Tf ₂ N] (1) + CO ₂ (2) system at 313.15 K	175
D8 Modeling solubility (P, T, x) data for [pmim][Tf ₂ N] (1) + CO ₂ (2) system at 323.15 K	176
D9 Modeling solubility (P, T, x) data for [pmim][Tf ₂ N] (1) + CO ₂ (2) system at 333.15 K	177
D10 Modeling solubility (P, T, x) data for [amim][Tf ₂ N] (1) + CO ₂ (2) system at 313.15 K	178
D11 Modeling solubility (P, T, x) data for [amim][Tf ₂ N] (1) + CO ₂ (2) system at 323.15 K	179
D12 Modeling solubility (P, T, x) data for [amim][Tf ₂ N] (1) + CO ₂ (2) system at 333.15 K	180
D13 Modeling solubility (P, T, x) data for [4mbp][BF ₄] (1) + CO ₂ (2) system at 313.15 K	181
D14 Modeling solubility (P, T, x) data for [4mbp][BF ₄] (1) + CO ₂ (2) system at 323.15 K	182

TABLE		PAGE
D15	Modeling solubility (P, T, x) data for [4mbp][BF ₄] (1) + CO ₂ (2) system at 333.15 K	183
E1	Experimental fugacity of CO ₂ in [S ₂₂₂][Tf ₂ N] at 313.15 K	184
E2	Experimental fugacity of CO ₂ in [S ₂₂₂][Tf ₂ N] at 323.15 K	185
E3	Experimental fugacity of CO ₂ in [S ₂₂₂][Tf ₂ N] at 333.15 K	186
E4	Experimental fugacity of CO ₂ in [deme][Tf ₂ N] at 313.15 K	188
E5	Experimental fugacity of CO ₂ in [deme][Tf ₂ N] at 323.15 K	189
E6	Experimental fugacity of CO ₂ in [deme][Tf ₂ N] at 333.15 K	190
E7	Experimental fugacity of CO ₂ in [pmim][Tf ₂ N] at 313.15 K	192
E8	Experimental fugacity of CO ₂ in [pmim][Tf ₂ N] at 323.15 K	193
E9	Experimental fugacity of CO ₂ in [pmim][Tf ₂ N] at 333.15 K	194
E10	Experimental fugacity of CO ₂ in [amim][Tf ₂ N] at 313.15 K	196
E11	Experimental fugacity of CO ₂ in [amim][Tf ₂ N] at 323.15 K	197
E12	Experimental fugacity of CO ₂ in [amim][Tf ₂ N] at 333.15 K	198
E13	Experimental fugacity of CO ₂ in [4mbp][BF ₄] at 313.15 K	200
E14	Experimental fugacity of CO ₂ in [4mbp][BF ₄] at 323.15 K	201
E15	Experimental fugacity of CO ₂ in [4mbp][BF ₄] at 333.15 K	202

LIST OF FIGURES

FIGURE	PAGE
2.1 Ionic configuration of inorganic salts (left) and ionic liquids (right)	5
2.2 Some cations and anions present in ionic liquids	7
2.3 Plots showing the melting and clearing temperatures observed on heating of (a) $[C_n\text{-mim}][PF_6]$, (b) $[C_n\text{-py}][PF_6]$, (c) $[C_n\text{-3-Mepy}][PF_6]$, and (d) $[C_n\text{-4-Mepy}][PF_6]$	9
2.4 Comparison of experimental densities of ionic liquids with calculated values	11
2.5 Viscosities of imidazolium- and pyridinium-based ionic liquids with butyl chain length and different anions at 298.15 and 323.15 K (25 and 50 °C)	13
2.6 Viscosities of ionic liquids as a function of temperature: (●), $[bmim][PF_6]$; (○), $[bmim][Tf_2N]$; (■), $[bmim][BF_4]$; (□), $[N_{4111}][Tf_2N]$; (▲), $[emim][Tf_2N]$; (Δ), $[emim][EtSO_4]$	13
2.7 Viscosity of ionic liquids as a function of pressure at 323.15 K (50 °C)	14
2.8 The Kugelrohr oven and distillation apparatus	17
2.9 Surface tensions (mJ/m^2) of several ionic liquids as a function of temperature	19
2.10 Some commonly used ionic liquids and the level of water miscibility	24
2.11 Applications of ionic liquids	25
2.12 The schematic of the stoichiometric apparatus	26
2.13 The schematic of the pressure drop apparatus	27
2.14 The IGA003 gravimetric analyzer	29
2.15 The schematic of the intelligent gravimetric analyzer	29

FIGURE	PAGE
2.16 The schematic of Rubotherm magnetically coupled microbalance	30
2.17 The schematic of quartz crystal microbalance apparatus	31
2.18 CO ₂ solubility in [bmim][PF ₆] at 25 °C	33
2.19 Proposed mechanism for enhanced CO ₂ solubility in imidazolium acetate	47
2.20 CO ₂ solubility in [bmim][PF ₆] at 283.15, 298.15, and 273.15 K (10, 25 and 50 °C)	49
2.21 The CO ₂ solubility as a function of pressure up to 28.98 bar in ■ [C ₄ py][Tf ₂ N], and × [C ₁₂ py][Tf ₂ N] at 298.15 K	50
2.22 The CO ₂ solubility in [C ₄ py][Tf ₂ N] at: ■ 298.15 K (25 °C), ▲ 313.15 K (40 °C) and × 333.15 K (60 °C)	50
2.23 Henry's law constants for CO ₂ in various ionic liquids at 333.15 K (60 °C)	52
2.24 The effect of alkyl chain length of cations on the CO ₂ solubility in [C ₄ py][Tf ₂ N], [C ₈ py][Tf ₂ N], [C ₁₀ py][Tf ₂ N] and [C ₁₂ py][Tf ₂ N] at 298.15 K (25 °C)	53
2.25 Two types of molecular clusters or cells of binary liquid mixtures	64
3.1 The DMA 4500 density meter	73
3.2 Schematic diagram of Hiden Isochema IGA-003 gravimetric microbalance	74
3.3 IGA-003 configuration set for static gas operation	75
4.1 Liquid density of the studied ionic liquids at temperatures ranging from 278.15 K to 353.15 K: ●, [S ₂₂₂][Tf ₂ N]; ○, [deme][Tf ₂ N]; ▼, [pmim][Tf ₂ N]; Δ, [amim][Tf ₂ N]; ■, [4mbp][BF ₄]	87

FIGURE	PAGE
4.2 Absorption of CO ₂ in [bmim][PF ₆] at 323.15 K compared to the solubility data obtained in literature: ●, this work; ○, Shiflett and Yokozeki (2005); ▼, Anthony <i>et al.</i> (2002)	88
4.3 Comparison of measured isothermal solubility data of CO ₂ in different ionic liquids: ●, [S ₂₂₂][Tf ₂ N]; ○, [deme][Tf ₂ N]; ▼, [pmim][Tf ₂ N]; Δ, [amim][Tf ₂ N]; ■, [4mbp][BF ₄]; red, at 313.15 K; blue, at 323.15 K; green, at 333.15 K	91
4.4 Comparison of measured isothermal solubility data of CO ₂ in different ionic liquids at 313.15 K: ●, [S ₂₂₂][Tf ₂ N]; ○, [deme][Tf ₂ N]; ▼, [pmim][Tf ₂ N]; Δ, [amim][Tf ₂ N]; ■, [4mbp][BF ₄]	93
4.5 Comparison of measured isothermal solubility data of CO ₂ in different ionic liquids at 323.15 K: ●, [S ₂₂₂][Tf ₂ N]; ○, [deme][Tf ₂ N]; ▼, [pmim][Tf ₂ N]; Δ, [amim][Tf ₂ N]; ■, [4mbp][BF ₄]	93
4.6 Comparison of measured isothermal solubility data of CO ₂ in different ionic liquids at 333.15 K: ●, [S ₂₂₂][Tf ₂ N]; ○, [deme][Tf ₂ N]; ▼, [pmim][Tf ₂ N]; Δ, [amim][Tf ₂ N]; ■, [4mbp][BF ₄]	94
4.7 Comparison between the solubility of CO ₂ in the studied ionic liquids and others published in the literature at 323.15 K: black ●, HEAF; red ●, HEL; green ▼, THEAA; yellow ▲, HEF; blue ■, HEAL; pink ■, HEA; cyan ◆, THEAL; gray ◆, HEAA; dark red ▲, [4mbp][BF ₄]; dark green ▼, [bmim][BF ₄]; dark yellow ●, [bmim][PF ₆]; dark blue ●, [S ₂₂₂][Tf ₂ N]; dark pink ▼, [amim][Tf ₂ N]; dark cyan ▲, [pmim][Tf ₂ N]; dark gray ■, [bmim][Tf ₂ N]; black ■, [deme][Tf ₂ N]; red ◆, [hmim][Tf ₂ N]; green ◆, [bmpyrr][eFAP]; yellow ●, [hmim][eFAP]; blue ●, [bmim][Ac]	96

FIGURE	PAGE
4.8 Comparison between the solubility of CO ₂ in [deme][Tf ₂ N] and other ammonium-based ionic liquids in the literature at 313.15 K: black ●, HHEMEA; red ●, HHEMEL; green ▼, BHEAL; yellow ▲, HEL; blue ■, BHEAA; pink ■, HEA; cyan ◆, [deme][Tf ₂ N]	100
4.9 Comparison of the solubility of CO ₂ in [deme][Tf ₂ N] with the existing ionic liquids containing ammonium and phosphonium cations in the literature at 333.15 K: black ●, [choline][Tf ₂ N]; red ●, [N ₄₁₁₁][Tf ₂ N]; green ▼, [deme][Tf ₂ N]; yellow ▲, [P ₍₁₄₎₆₆₆][Tf ₂ N]	102
4.10 Comparison of the solubility of CO ₂ in ionic liquids studied in our group at 323.15 K: black ●, [4mbp][BF ₄]; red ●, [bmim][TfO]; green ▼, [bmim][DPH]; yellow ▲, [(OMe) ₂ Im][Tf ₂ N]; blue ■, [S ₂₂₂][Tf ₂ N]; pink ■, [amim][Tf ₂ N]; cyan ◆, [1b1mp][Tf ₂ N]; gray ◆, [pmim][Tf ₂ N]; dark red ▲, [(OEt) ₂ Im][Tf ₂ N]; dark green ▼, [deme][Tf ₂ N]	103
4.11 P-x diagram of the system [S ₂₂₂][Tf ₂ N] and CO ₂ for different temperatures. Symbols represent the experimental data: ●, at 313.15 K; ○, at 323.15 K; and ▼, at 333.15 K. Lines represent the estimations by the standard PR-EoS: solid line, at 313.15 K; dotted line, at 323.15 K; and dashed line, at 333.15 K	106
4.12 P-x diagram of the system [deme][Tf ₂ N] and CO ₂ for different temperatures. Symbols represent the experimental data: ●, at 313.15 K; ○, at 323.15 K; and ▼, at 333.15 K. Lines represent the estimations by the standard PR-EoS: solid line, at 313.15 K; dotted line, at 323.15 K; and dashed line, at 333.15 K	107

FIGURE	PAGE
<p>4.13 P-x diagram of the system [pmim][Tf₂N] and CO₂ for different temperatures. Symbols represent the experimental data: ●, at 313.15 K; ○, at 323.15 K; and ▼, at 333.15 K. Lines represent the estimations by the standard PR-EoS: solid line, at 313.15 K; dotted line, at 323.15 K; and dashed line, at 333.15 K</p>	107
<p>4.14 P-x diagram of the system [amim][Tf₂N] and CO₂ for different temperatures. Symbols represent the experimental data: ●, at 313.15 K; ○, at 323.15 K; and ▼, at 333.15 K. Lines represent the estimations by the standard PR-EoS: solid line, at 313.15 K; dotted line, at 323.15 K; and dashed line, at 333.15 K</p>	108
<p>4.15 P-x diagram of the system [4mbp][BF₄] and CO₂ for different temperatures. Symbols represent the experimental data: ●, at 313.15 K; ○, at 323.15 K; and ▼, at 333.15 K. Lines represent the estimations by the standard PR-EoS: solid line, at 313.15 K; dotted line, at 323.15 K; and dashed line, at 333.15 K</p>	108
<p>4.16 Comparison of isothermal solubility data of CO₂ in different ionic liquids: ●, [S₂₂₂][Tf₂N]; ○, [deme][Tf₂N]; ▼, [pmim][Tf₂N]; △, [amim][Tf₂N]; and ■, [4mbp][BF₄]; red, at 313.15 K; blue, at 323.15 K; and green, at 333.15 K. Lines represent the estimations by the standard PR-EoS</p>	109
<p>4.17 P-x diagram of the system [S₂₂₂][Tf₂N] and CO₂ for different temperatures. Symbols represent the experimental data: ●, at 313.15 K; ○, at 323.15 K; and ▼, at 333.15 K. Lines represent the estimations by the standard SRK-EoS: solid line, at 313.15 K; dotted line, at 323.15 K; and dashed line, at 333.15 K</p>	111

FIGURE	PAGE
4.18 P-x diagram of the system [deme][Tf ₂ N] and CO ₂ for different temperatures. Symbols represent the experimental data: ●, at 313.15 K; ○, at 323.15 K; and ▼, at 333.15 K. Lines represent the estimations by the standard SRK-EoS: solid line, at 313.15 K; dotted line, at 323.15 K; and dashed line, at 333.15 K	111
4.19 P-x diagram of the system [pmim][Tf ₂ N] and CO ₂ for different temperatures. Symbols represent the experimental data: ●, at 313.15 K; ○, at 323.15 K; and ▼, at 333.15 K. Lines represent the estimations by the standard SRK-EoS: solid line, at 313.15 K; dotted line, at 323.15 K; and dashed line, at 333.15 K	112
4.20 P-x diagram of the system [amim][Tf ₂ N] and CO ₂ for different temperatures. Symbols represent the experimental data: ●, at 313.15 K; ○, at 323.15 K; and ▼, at 333.15 K. Lines represent the estimations by the standard SRK-EoS: solid line, at 313.15 K; dotted line, at 323.15 K; and dashed line, at 333.15 K	112
4.21 P-x diagram of the system [4mbp][BF ₄] and CO ₂ for different temperatures. Symbols represent the experimental data: ●, at 313.15 K; ○, at 323.15 K; and ▼, at 333.15 K. Lines represent the estimations by the standard SRK-EoS: solid line, at 313.15 K; dotted line, at 323.15 K; and dashed line, at 333.15 K	113
4.22 Comparison of isothermal solubility data of CO ₂ in different ionic liquids: ●, [S ₂₂₂][Tf ₂ N]; ○, [deme][Tf ₂ N]; ▼, [pmim][Tf ₂ N]; Δ, [amim][Tf ₂ N]; and ■, [4mbp][BF ₄]; red, at 313.15 K; blue, at 323.15 K; and green, at 333.15 K. Lines represent the estimations by the standard SRK-EoS	113

FIGURE	PAGE
4.23 P-x diagram of the system [S ₂₂₂][Tf ₂ N] and CO ₂ for different temperatures. Symbols represent the experimental data: ●, at 313.15 K; ○, at 323.15 K; and ▼, at 333.15 K. Lines represent the estimations by the SRK with quadratic mixing rules: solid line, at 313.15 K; dotted line, at 323.15 K; and dashed line, at 333.15 K	116
4.24 P-x diagram of the system [deme][Tf ₂ N] and CO ₂ for different temperatures. Symbols represent the experimental data: ●, at 313.15 K; ○, at 323.15 K; and ▼, at 333.15 K. Lines represent the estimations by the SRK with quadratic mixing rules: solid line, at 313.15 K; dotted line, at 323.15 K; and dashed line, at 333.15 K	116
4.25 P-x diagram of the system [pmim][Tf ₂ N] and CO ₂ for different temperatures. Symbols represent the experimental data: ●, at 313.15 K; ○, at 323.15 K; and ▼, at 333.15 K. Lines represent the estimations by the SRK with quadratic mixing rules: solid line, at 313.15 K; dotted line, at 323.15 K; and dashed line, at 333.15 K	117
4.26 P-x diagram of the system [amim][Tf ₂ N] and CO ₂ for different temperatures. Symbols represent the experimental data: ●, at 313.15 K; ○, at 323.15 K; and ▼, at 333.15 K. Lines represent the estimations by the SRK with quadratic mixing rules: solid line, at 313.15 K; dotted line, at 323.15 K; and dashed line, at 333.15 K	117
4.27 P-x diagram of the system [4mbp][BF ₄] and CO ₂ for different temperatures. Symbols represent the experimental data: ●, at 313.15 K; ○, at 323.15 K; and ▼, at 333.15 K. Lines represent the estimations by the SRK with quadratic mixing rules: solid line, at 313.15 K; dotted line, at 323.15 K; and dashed line, at 333.15 K	118

FIGURE	PAGE
4.28 Comparison of isothermal solubility data of CO ₂ in different ionic liquids: ●, [S ₂₂₂][Tf ₂ N]; ○, [deme][Tf ₂ N]; ▼, [pmim][Tf ₂ N]; Δ, [amim][Tf ₂ N]; and ■, [4mbp][BF ₄]; red, at 313.15 K; blue, at 323.15 K; and green, at 333.15 K. Lines represent the estimations by the SRK with quadratic mixing rules	118
4.29 P-x diagram of the system [S ₂₂₂][Tf ₂ N] and CO ₂ for different temperatures. Symbols represent the experimental data: ●, at 313.15 K; ○, at 323.15 K; and ▼, at 333.15 K. Lines represent the estimations by the NRTL: solid line, at 313.15 K; dotted line, at 323.15 K; and dashed line, at 333.15 K	121
4.30 P-x diagram of the system [deme][Tf ₂ N] and CO ₂ for different temperatures. Symbols represent the experimental data: ●, at 313.15 K; ○, at 323.15 K; and ▼, at 333.15 K. Lines represent the estimations by the NRTL: solid line, at 313.15 K; dotted line, at 323.15 K; and dashed line, at 333.15 K	121
4.31 P-x diagram of the system [pmim][Tf ₂ N] and CO ₂ for different temperatures. Symbols represent the experimental data: ●, at 313.15 K; ○, at 323.15 K; and ▼, at 333.15 K. Lines represent the estimations by the NRTL: solid line, at 313.15 K; dotted line, at 323.15 K; and dashed line, at 333.15 K	122
4.32 P-x diagram of the system [amim][Tf ₂ N] and CO ₂ for different temperatures. Symbols represent the experimental data: ●, at 313.15 K; ○, at 323.15 K; and ▼, at 333.15 K. Lines represent the estimations by the NRTL: solid line, at 313.15 K; dotted line, at 323.15 K; and dashed line, at 333.15 K	122

FIGURE	PAGE
4.33 P-x diagram of the system [4mbp][BF ₄] and CO ₂ for different temperatures. Symbols represent the experimental data: ●, at 313.15 K; ○, at 323.15 K; and ▼, at 333.15 K. Lines represent the estimations by the NRTL: solid line, at 313.15 K; dotted line, at 323.15 K; and dashed line, at 333.15 K	123
4.34 Comparison of isothermal solubility data of CO ₂ in different ionic liquids: ●, [S ₂₂₂][Tf ₂ N]; ○, [deme][Tf ₂ N]; ▼, [pmim][Tf ₂ N]; Δ, [amim][Tf ₂ N]; and ■, [4mbp][BF ₄]; red, at 313.15 K; blue, at 323.15 K; and green, at 333.15 K. Lines represent the estimations by the NRTL	123
4.35 Henry's law constants for CO ₂ in [S ₂₂₂][Tf ₂ N], [deme][Tf ₂ N], [pmim][Tf ₂ N], [amim][Tf ₂ N] and [4mbp][BF ₄] at 313.15, 323.15 and 333.15 K	126
E1 Determining the Henry's law constant for CO ₂ in [S ₂₂₂][Tf ₂ N]	186
E2 Determining the enthalpy of absorption for CO ₂ in [S ₂₂₂][Tf ₂ N]	187
E3 Determining the entropy of absorption for CO ₂ in [S ₂₂₂][Tf ₂ N]	187
E4 Determining the Henry's law constant for CO ₂ in [deme][Tf ₂ N]	190
E5 Determining the enthalpy of absorption for CO ₂ in [deme][Tf ₂ N]	191
E6 Determining the entropy of absorption for CO ₂ in [deme][Tf ₂ N]	191
E7 Determining the Henry's law constant for CO ₂ in [pmim][Tf ₂ N]	194

FIGURE		PAGE
E8	Determining the enthalpy of absorption for CO ₂ in [pmim][Tf ₂ N]	195
E9	Determining the entropy of absorption for CO ₂ in [pmim][Tf ₂ N]	195
E10	Determining the Henry's law constant for CO ₂ in [amim][Tf ₂ N]	198
E11	Determining the enthalpy of absorption for CO ₂ in [amim][Tf ₂ N]	199
E12	Determining the entropy of absorption for CO ₂ in [amim][Tf ₂ N]	199
E13	Determining the Henry's law constant for CO ₂ in [4mbp][BF ₄]	202
E14	Determining the enthalpy of absorption for CO ₂ in [4mbp][BF ₄]	203
E15	Determining the entropy of absorption for CO ₂ in [4mbp][BF ₄]	203